Influence of Atmospheric Variability on Transonic Aeroelasticity

S. Marques* and K. J. Badcock†

Department of Engineering, University of Liverpool, Liverpool, UK, L69 3GH

I. NOMENCLATURE

Symbols

A	Jacobian matrix
b	Optimisation problem constraints
$\mathcal{C}$	Cost Function for Interval Optimisation problem
C_L	Lift coefficient
C_L	Drag coefficient
I	Moment of inertia
θ	Vector of random parameters/optimisation variables
c	Speed of Sound
p	Eigenvector
$\mathbf{R}$	Residual vector of the fluid and/or structural model
S	Schur complement matrix
S_A	Wing area
L	Lift
W	Weight
$\mathbf{w}$	Vector of fluid and/or structural unknowns

Greek

λ	Eigenvalue
ϕ	Mode shape vector
μ	Bifurcation parameter (altitude)
ρ	Atmospheric density
θ	m-dimensional vector containing the m uncertain structural parameters

Subscripts or superscripts

f	Fluid model
s	Structural model
0	Equilibrium
xx, yy, zz	Axis for moment of inertia
$\hat{\theta}$	Mean value of θ

*Research Associate Corresponding author Tel: +44 (0) 1517944889 Fax: +44 (0) 151794848.
†Professor

II. Introduction

Flutter testing is expensive, arduous and subject to several parameters difficult to control and predict, such as structural and meteorologic variability. Typical aerodynamic and aeroelastic simulations use the International Standard Atmosphere to represent input flow conditions. Progress has been made in the development of fast (relative to time domain analysis), Euler based eigenvalue flutter stability prediction methods.[1] The approach, based on an eigenvalue solution of a coupled CFD-FEM system, reduced the cost of non-deterministic flutter calculations at transonic conditions.[3] As part of an effort to evaluate the influence of structural variability, stochastic tools to evaluate the effects of structural variability have been coupled with this eigenvalue method.[3] This paper proposes proposes a methodology to evaluate and propagate the influence of atmospheric variability on aeroelastic stability using CFD level aerodynamics.

The atmosphere can be described as dynamic, complex and chaotic system. The range of meteorologic conditions an aircraft can find can be distinct and have an impact on performance. Variability in the atmosphere has many sources and different mechanisms and interactions contribute towards it.[19] These range from solar activity fluctuations, interactions with the oceans, atmospheric circulations, seasonal variations, to name a few. In this study, the influence of variability of thermodynamic properties of the atmosphere on the flutter boundary is investigated. The approach to propagate atmospheric variability is to compute the effects of temperature and density variations on cruise velocity and trim settings for straight and level flight conditions.

In this paper, meteorologic measurements are used to construct a non-deterministic representation of the variability of relevant atmospheric properties. Of particular interest to perform flutter matched calculations are variations of the temperature, pressure and density. The atmospheric variability effects on flutter are analysed by Monte-Carlo methods and interval analysis, coupled with a deterministic eigenvalue aeroelastic solver based on the Schur Complement formulation.[1] The variability is propagated to the analysis through the fluid jacobian and a bifurcation parameter such as dynamic pressure or altitude. Flutter calculations on the Goland and MDO wings are used as test problems to demonstrate the approach.

III. Aeroelastic Stability Formulation

The semi-discrete form of the coupled CFD-FEM system is written as

$$\frac{d\mathbf{w}}{dt} = \mathbf{R}(\mathbf{w}, \mu) \tag{1}$$

where

$$\mathbf{w} = [\mathbf{w}_f, \mathbf{w}_s]^T \tag{2}$$

is a vector containing the fluid unknowns ($\mathbf{w}_f$) and the structural unknowns ($\mathbf{w}_s$), and

$$\mathbf{R} = [\mathbf{R}_f, \mathbf{R}_s]^T \tag{3}$$

is a vector containing the fluid residual ($\mathbf{R}_f$) and the structural residual ($\mathbf{R}_s$). In this paper, the fluid model is given by the Euler equations, whereas the structural model is defined by the following scalar equations

$$\frac{d^2\alpha_i}{dt^2} + D_i\frac{d\alpha_i}{dt} + \omega_i^2\alpha_i = \frac{\rho_\infty}{\rho_w}\phi_i^T f_s \tag{4}$$

where α_i are the generalised coordinates, ϕ_i represents the mode shapes extracted from the finite element model, D_i are the damping coefficients, f_s is the vector of aerodynamic forces at the structural grid points and ρ_∞/ρ_w is the density ratio between air and the wing; ρ_∞ depends on the altitude, i.e. $\rho_\infty = f(\mu)$. The value for a particular altitude can be defined from ISA relations or is obtained from direct measurements, $\rho_\infty = \rho_i$.

The residual depends on a parameter μ which is independent of $\mathbf{w}$, in this paper the parameter corresponds to altitude. An equilibrium $\mathbf{w}_0$ of this system satisfies $\mathbf{R}(\mathbf{w}_0, \mu) = \mathbf{0}$.

The linear stability of equilibria of equation (1) is determined by eigenvalues of the Jacobian matrix $A = \partial\mathbf{R}/\partial\mathbf{w}$. In the current work a stability analysis is done based on the coupled system Jacobian matrix which includes the Jacobian of the CFD residual with respect to the CFD and structural unknowns. The

calculation of the Jacobian A is most conveniently done by partitioning the matrix as

$$A = \begin{bmatrix} \frac{\partial \mathbf{R}_f}{\partial \mathbf{w}_f} & \frac{\partial \mathbf{R}_f}{\partial \mathbf{w}_s} \\ \frac{\partial \mathbf{R}_s}{\partial \mathbf{w}_f} & \frac{\partial \mathbf{R}_s}{\partial \mathbf{w}_s} \end{bmatrix} = \begin{bmatrix} A_{ff} & A_{fs} \\ A_{sf} & A_{ss} \end{bmatrix}. \tag{5}$$

Details of the implementation of the Euler and structural equations and Jacobian calculation can be found in references[5] and.[6]

In the current work, and as is conventional in aircraft aeroelasticity, the structure is modelled by a small number of modes, and so the number of the fluid unknowns is far higher than the structural unknowns. This means that the Jacobian matrix has a large, but sparse, block A_{ff} surrounded by thin strips for A_{fs} and A_{sf}. As described in reference[1] the stability calculation is formulated as an eigenvalue problem, focussing on eigenvalues of the coupled system that originate from the uncoupled block A_{ss}.

Write the coupled system eigenvalue problem as

$$\begin{bmatrix} A_{ff} & A_{fs} \\ A_{sf} & A_{ss} \end{bmatrix} \mathbf{p} = \lambda \mathbf{p} \tag{6}$$

where $\mathbf{p} - [\mathbf{p}_f, \mathbf{p}_s]^T$ and λ are the complex eigenvector and eigenvalue respectively. The eigenvalue λ (assuming it is not an eigenvalue of A_{ff}) satisfies[21] the nonlinear eigenvalue problem

$$S(\lambda)\mathbf{p}_s = \lambda \mathbf{p}_s \tag{7}$$

where $S(\lambda) = A_{ss} - A_{sf}(A_{ff} - \lambda I)^{-1} A_{fs}$.

The nonlinear equation (7) is solved using Newton's method. Each iteration requires the formation of the residual, $S(\lambda)\mathbf{p}_s - \lambda \mathbf{p}_s$ and its Jacobian matrix. The calculation of the correction matrix, $A_{sf}(A_{ff} - \lambda I)^{-1} A_{fs}$, is required to form the Jacobian matrix with respect to $\mathbf{p}_s$ and λ. This can be achieved through $2n$ solutions of a linear system against $A_{ff} - \lambda I$, one for each column of A_{fs} with n being the number of normal modes retained. These solutions are then multiplied against A_{sf}. Now, for each value of the bifurcation parameter, there are multiple solutions of the nonlinear system in equation (7), and so the cost of forming the correction matrix at each Newton step, for each solution and for a range of structural parameters becomes too high. To overcome this the expansion

$$(A_{ff} - \lambda I)^{-1} = A_{ff}^{-1} + \lambda A_{ff}^{-2} + \lambda^2 A_{ff}^{-3} + ... \tag{8}$$

is used where λ must be small for the series to converge. Note that this assumption is not restrictive since we assume that the eigenvalue we are calculating is a small change from the eigenvalue λ_0 of A_{ss}. Then λ_0 can be used as a shift to the full system eigenvalue problem by replacing A_{ff} by $A_{ff} - \lambda_0 I$ and A_{ss} by $A_{ss} - \lambda_0$. This modifies the nonlinear eigenvalue problem in equation (7) by redefining $S(\lambda) = (A_{ss} - \lambda_0 I - \lambda I) - A_{sf}(A_{ff} - \lambda_0 I - \lambda I)^{-1} A_{fs}$. The series approximation then becomes

$$(A_{ff} - \lambda_0 I - \lambda I)^{-1} = (A_{ff} - \lambda_0 I)^{-1} + \lambda (A_{ff} - \lambda_0 I)^{-2} + \lambda^2 (A_{ff} - \lambda_0 I)^{-3} + ... \tag{9}$$

When the shifted problem is solved for λ, the eigenvalue of the original system is then $\lambda_0 + \lambda$. The terms $(A_{ff} - \lambda_0 I)^{-1} A_{fs}, \lambda (A_{ff} - \lambda_0 I)^{-2} A_{fs}$ can be pre-computed to yield the series approximation which can then be evaluated for any λ at virtually no computational cost.

This method is referred to as the Schur method. Two forms are available. In both cases the series approximation is used for approximating the Jacobian matrix of the residual from equation (7). For the residual the evaluation of $S(\lambda)\mathbf{p}_s - \lambda \mathbf{p}_s$ can be made based on an exact evaluation (referred to as *full* in this paper) which requires the solution of one linear system against the right hand side $A_{fs}\mathbf{p}_s$, or can use the series approximation (referred to as *series*) at virtually no additional cost after the series matrices are formed.

IV. Atmospheric Variability

Over the last 60 years there has been an increasing effort to measure and record physical properties of the atmosphere across the globe. This data has value not just for meteorological analysis, but is also

required to engineer air vehicles, such as re-entry capsules or airline cruisers. The type of data available includes measurements for pressure, temperature, temperature dew point, wind magnitude and direction, typically over a range of altitudes between 500 and 30000m and was obtained by radio-soundings.[2] Daily temperature and pressure measurements were extracted from time series data going back 25 years, which is twice as long as the typical solar cycle and more recent data sets have the advantage of increased altitude resolution. A total of over 8000 samples for temperature, density[a] and pressure over the altitude range were gathered, for a variety of locations and altitudes. As an example, data obtained from a measuring station in central U.S. was used to calculate histograms of the deviation from ISA values at 8200m as shown in fig.1. Tables1 and 2 show the amplitude in density and speed of sound values, whereas fig.2 are scatter plots of the measurement for five reference locations and altitudes. Measurements show clear differences in amplitude observed, distribution and even correlations between the density and speed of sound.

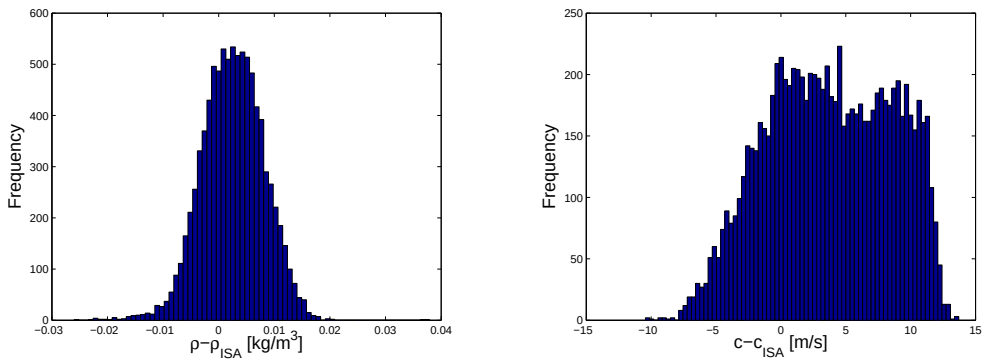

Figure 1. Histogram for density and speed of sound based on atmospheric measurements obtained at 8200m

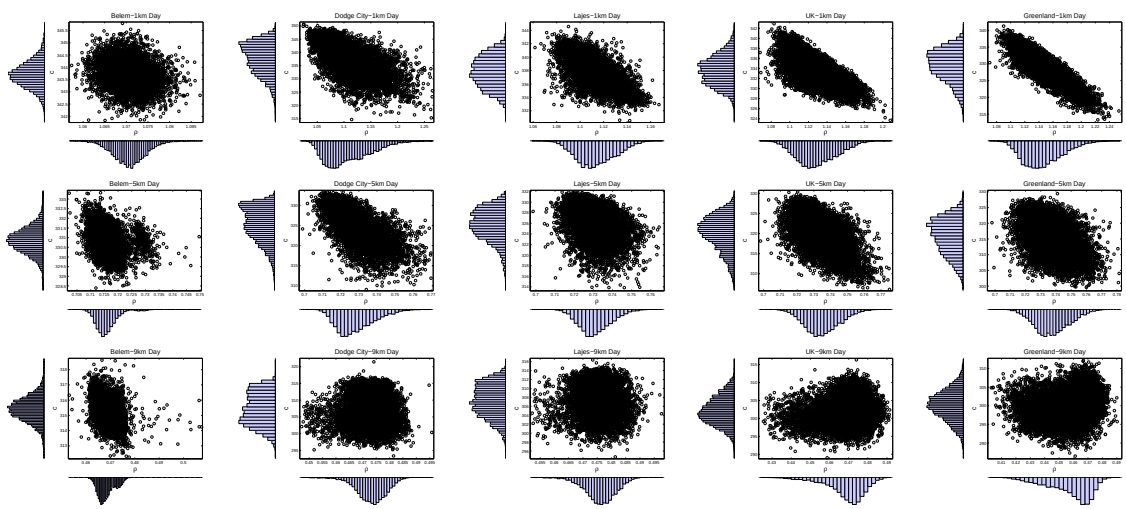

Figure 2. Histogram for density and speed of sound based on atmospheric measurements - day

V. Propagating Atmospheric Variability

A. Flight Dynamics

To study the influence of the atmospheric variability, it is necessary to understand how changes in pressure, density and temperature affect a given aircraft. In this work all flutter calculations assume straight and level flight, therefore the impact of atmospheric variability in this condition is first examined. Consider an

[a] the density is calculated using the perfect gas law, from measured temperature and pressure

Altitude $[km]$	Belém	Dodge City	Greenland	Lajes	UK
1	0.0297	0.2410	0.1830	0.1054	0.1398
3	0.0371	0.1252	0.1223	0.0756	0.1000
5	0.0475	0.0709	0.0835	0.0658	0.0770
7	0.0594	0.0499	0.0670	0.0499	0.0579
9	0.0543	0.0485	0.0873	0.0453	0.0659
11	0.0504	0.0779	0.0880	0.0483	0.0840

Table 1. Diurnal Amplitudes for density based on observations- values in kg/m^3

Altitude $[km]$	Belém	Dodge City	Greenland	Lajes	UK
1	3.8561	36.1584	28.3288	12.8284	19.0022
3	4.4318	26.3667	30.9420	16.7409	19.9598
5	4.8752	25.4966	29.3122	18.9053	24.0127
7	5.0168	26.2700	34.6376	20.7140	26.2512
9	5.9666	26.3629	28.1431	23.2644	26.4954
11	6.2056	22.4906	29.1535	17.0339	22.3862

Table 2. Diurnal Amplitudes for speed of sound based on observations - values in m/s

aircraft flying in straight and level flight:

$$W = L = \frac{1}{2}\rho_\infty(\gamma R T_\infty) M_\infty^2 S_A C_L \tag{10}$$

$$T = D = \frac{1}{2}\rho_\infty(\gamma R T_\infty) M_\infty^2 S_A C_D \tag{11}$$

To maintain straight and level flight and conditions in $\rho_\infty,\ T_\infty$ change, the pilot is required to change the trim settings of the aircraft in order to keep the forces in eq.10 balanced. To compute the new trim states for each combination of $\rho_\infty,\ T_\infty$, a Flight Dynamics analysis tool based on tabular data, CFD and sampling techniques, developed at the University of Liverpool is employed.[15,16] This approach is briefly summarised next.

Traditionally, flight dynamics calculations are based on aerodynamic data tables, containing aerodynamic forces and moments:

$$[C_L, C_D, C_m, C_Y, C_l, C_n]^T$$

representing wind axis coefficients of lift, drag, pitching-moment, side-force, rolling moment and yawing moment coefficient, respectively.[7,8] This information is provided from CFD analysis, however it is not practical to complete the whole table from CFD results, therefore a kriging and data-fusion sampling method was used to form the complete data set for flight dynamics analysis. With the aerodynamic tables populated, it is possible to compute time-optimal maneuvres based on pilot's control inputs. The optimal control aims to find a state-control pair, $x^*()$, $u^*()$, and possibly the final event time t_f that minimizes the cost function:[18]

$$J\left[x(), u(), t_0, t_f\right] = E\left(x(t_0), u(t_0), t_0, t_f\right) + \int_{t_0}^{t_f} F\left(x(t), u(t), t\right) \tag{12}$$

There are many different methods of solving the optimal control problems, in the current paper the commercially available codes DIDO and Matlab[14] are used. In DIDO, the total time history is divided into N segments, spaced using shifted Legendre-Gauss-Lobatto (LGL) rule.[9–11] The boundaries of each time segment are called nodes. the code exploits pseudo-spectral (PS) methods for solving the optimal control problems. For the problem of an aircraft optimal time maneuvre, the general 6-degree-of-freedom aircraft equations of motion detailed in Etkin[12] and Stevens and Lewis[13] serve as one of the constraints. The aircraft state vector consists of the position of the aircraft ($\mathbf{x}$, $\mathbf{y}$, $\mathbf{z}$), the standard Euler angles (ϕ, θ, ψ), the

velocity components in terms of Mach number and flow angles (M, α, β), and the body-axis components of the angular velocity vector ($\mathbf{p}$, $\mathbf{q}$, $\mathbf{r}$). The initial and final state parameters are fixed with trimmed flight conditions, but the rest of the maneuvre is out of trim conditions. The loads in the aircraft equations of motion are interpolated from the generated look-up tables.

1. *Flight Dynamics Reference Test Case*

To evaluate the effects of atmospheric variability, each combination of density and speed of sound formed an input to calculate a new trim state for the Ranger 2000 trainer aircraft. During the maneuvre altitude and Mach number are fixed. Details of the generation of the aerodynamic tables and aircraft model are given by Ghoreyshi *et al.*[16] and will not be given here. This is a mid-wing, tandem seat training aircraft powered by one turbofan engine with uninstalled thrust of 14190 N. The wing and fuselage are manufactured of composite material and the empennage is a metal T-tail design. The general dimensions of the aircraft are given in table 3. The vehicle flight control system consists of three conventional control surfaces: the elevator

length overall (m)	10.39
wing span (m)	10.46
wing area m^2	15.5
mean aerodynamic chord (mac) (m)	1.545
wing taper ratio	0.519
OEW (kg)	2586
MTOW(maximum) (kg)	3765

Table 3. Ranger 2000 Dimensions

at the tail, the rudder at the fin and left and right ailerons. Reference trim conditions were calculated based on ISA values at 8200m, velocity of 154m/s (corresponding to a Mach n. 0.5), this resulted in the trim settings shown in table 4:

Mach n.	α	δ_{elev}
0.50	2.3861°	1.1213°

Table 4. Trim settings for ISA conditions at 8200m, M0.5

The results from the trim calculations provide a basis for quantitative information of the variation likely to exist in the input parameters when computing flutter solutions. Hence, a set of angles of attack, velocities and elevator deflections were obtained from DIDO, as shown in fig.3. Note that the angle of attack in this case is dependent of the aircraft velocity, i.e. each velocity obtained has a corresponding angle of attack and elevator deflection, corresponding to a particular trim state. Furthermore, the velocity changes are mainly driven by changes in the speed of sound and this leads to a strong degree of correlation between angle of attack and velocity has illustrated by fig.4.

Another consequence of atmospheric variability are the changes on C_L and C_D, shown in fig.5, for the case illustrated here a variation of 15% and 4% were found for C_L and C_D, respectively.

B. Flutter Parameter Inputs

The flight dynamics analysis provides two types of additional parameters, angle of attack and control surface deflections. The variation of such quantities is propagated through the CFD analysis. Changes in density have a direct effect on eq.4, modifying the mass ratio and therefore the influence of the fluid on the structure. Finally, the velocity changes due to fluctuations in the speed of sound are relevant, since it will modify the

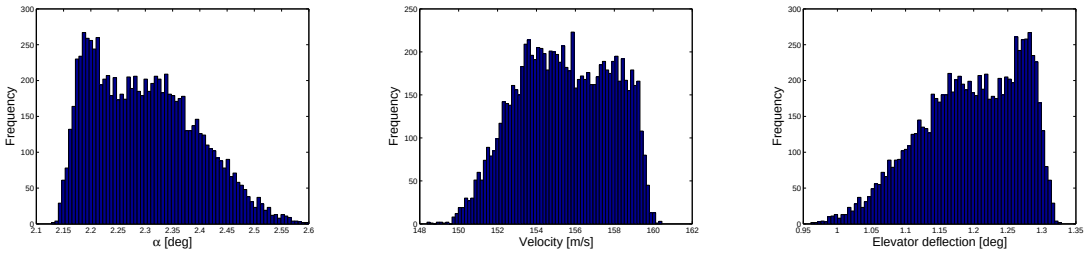

Figure 3. Histograms for trimmed aircraft solutions at 8200m - 9000 samples

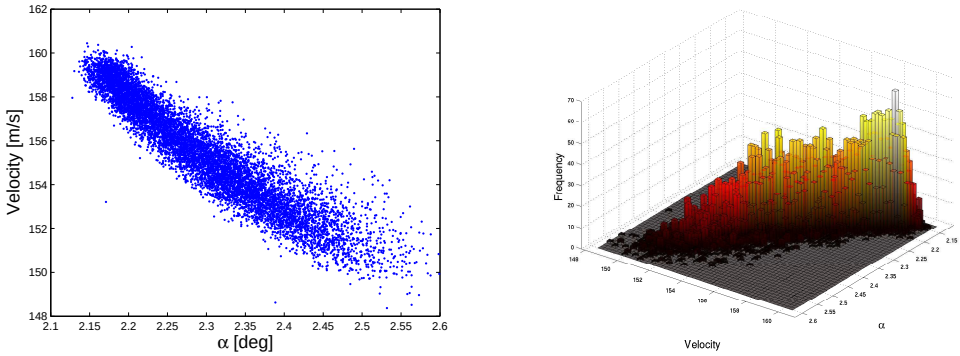

Figure 4. Velocity correlation with angle of attack at 8200m - 9000 samples

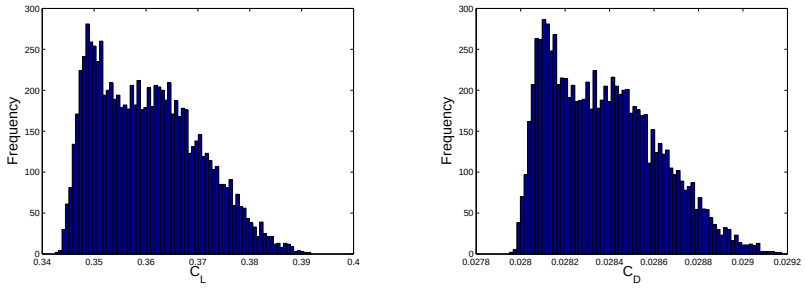

Figure 5. Histograms for trimmed aircraft solutions at 8200m - 9000 samples

frequency through the non-dimensionalisation process. The diagram in fig.6 summarises the steps to generate the set of inputs that can be used in flutter analyses.

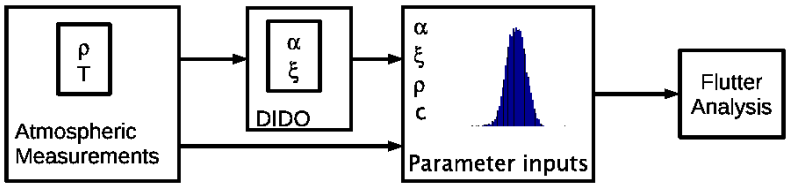

Figure 6. Process to propagate atmospheric variability

C. Flutter Uncertainty Quantification

1. *Monte-Carlo*

In a Monte Carlo process a subset of the initial measured data was selected, containing 1500 samples. These were used to compute 1500 different trim states. In the current work this requires recomputing the steady state for each condition, this result together with the input velocity for the non-dimensionalisation of the frequency and mass ratio are used for the aeroelastic calculations. The respective response values, the real and imaginary parts of the aeroelastic eigenvalues, λ_i (which denotes either the real or imaginary part of the ith eigenvalue) are evaluated using the Schur method as described in previous sections. The mean values and standard deviation of the eigenvalues can be directly evaluated from the scatter of the computed values.

2. *Interval Analysis*

An interval analysis defines a range for the uncertain parameters, and then computes the possible range for the aeroelastic eigenvalues.[3] To remain true to the inputs generated from observations, i.e. keeping the combinations of speed of sound, angle of attack and density within realistic limits of the samples already generated, additional constraints were added to limit the range of values the uncertain parameter could take, these are shown in fig.8. The interval flutter problem is expressed as:

$$\begin{cases} [\underline{\lambda}(\theta)_i, \overline{\lambda}(\theta)_i] & = [min(Re(\lambda_i)), max(Re(\lambda_i))] \\ S(\lambda_i)\mathbf{p}_s - \lambda_i \mathbf{p}_s & = 0, \\ \underline{\theta} \leq \theta \leq \overline{\theta} \\ g(\theta) < 0 \end{cases} \tag{13}$$

The index $()i$ indicates the critical mode, and the under and over bars indicate the lower and upper bounds of the variable, $g(\theta)$ represents additional constraints the variables must satisfy. A range for each of the variable structural parameters is chosen, and then an optimisation problem must be solved to find the resulting range on the critical eigenvalue. Solving this problem on such a parameter space with gradient based methods proved difficult due to the presence of multiple local minimum. Hence, in the current work the genetic optimisation algorithm in Matlab (ga), solves a constrained optimisation problem. This method requires the parameter constraints (i.e. intervals on θ) and a scalar objective function (which here corresponds the minimum or maximum real part of the critical eigenvalue).

VI. Results

A. Goland Wing

The Goland wing, shown in Fig. 7(a), has a chord of 1.8m and a span of 6m. It is a rectangular cantilevered wing with a 4% thick parabolic section. The structural model follows the description given in reference.[20] The CFD grid is block structured and uses an O-O topology. The fine grid has 250 thousand points and a coarse level was extracted from this grid, which has 40 thousand points. Grid refinement results reported previously in reference[1] showed that the coarse grid gives accurate aeroelastic damping predictions. Four

mode shapes were retained for the aeroelastic simulation, the first and second bending and torsion modes. The nominal conditions of this case correspond to M0.90 and $\alpha = 0°$, this is characterised by a strong schock-wave towards the trailing edge as illustrated by the CFD solution in fig.7. In order to validate and exercise

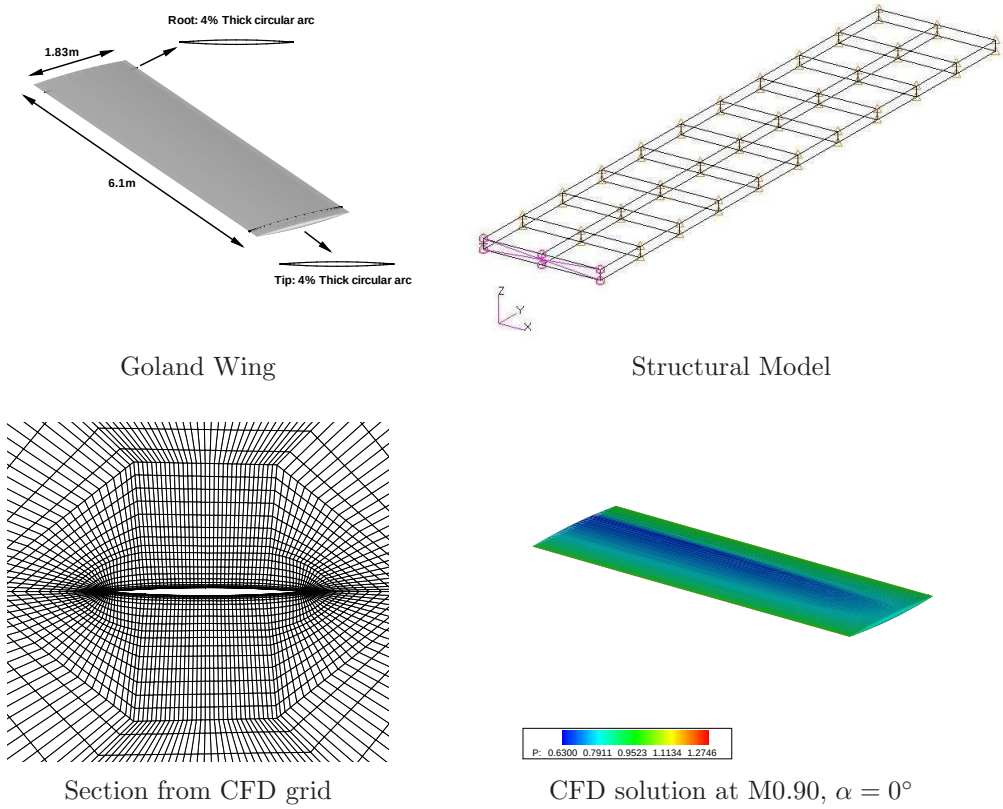

Figure 7. Goland Wing Geometry Model

the approach proposed in this work, the variations found for the Ranger aircraft are used as a reference in aeroelastic stability calculations of the Goland Wing. Hence, after solving the trimming problem a range of angles of attack about a nominal value can be specified (0° for the Goland Wing), representative of the influence of atmospheric variability, i.e. the angle of attack variation will have the same amplitude and distribution shown in fig.3 but about 0°. In total three random parameters are used: density and speed of sound, plus angle of attack (the elevator variation is not added since this case is a simple wing). Since the aeroelastic system looses stability when the real part of the eigenvalue becomes positive, the optimisation problem finds the parameter combination that maximize the real part of the eigenvalue. The samples from which the input parameters used for the MC analysis together with the constraints included in the definition of the optimisation problem are shown in fig.8 The MC analysis consisted of 1500 samples sets (i.e. an individual combination of M, α and ρ), whereas the interval analysis was limited to 100 function evaluations. The mode tracking for the nominal case is shown in fig.9. The wing looses stability at about 7000m , when the real part of mode 1 eigenvalue becomes positive. This mode was selected for the subsequent uncertainty analysis. Due to the computational cost, the MC analysis was only used for one altitude case, 8200m. The effects of atmospheric variability when using both techniques are give in fig.10. The MC results show a significant variation on the flutter onset; at the first altitude calculated the wing is already close to the instability point and results show that this type of variability might be sufficient to trigger flutter at this point. There is also a significant skewness on the sample distribution, as is also observed in fig.11, this is to be expected due to the symmetry of the Goland Wing and this case, i.e. when variation in α is likely to result in an increase in aerodynamic loading, leading to the loss of stability margin. The interval analysis also shows this skewness effect, the interval results are also conservative with respect to MC. This should be improved by enforcing tighter constraints on the bounds of the optimisation problem, however this may not be desirable for flutter computations. When using the interval analysis, atmospheric variability based on the

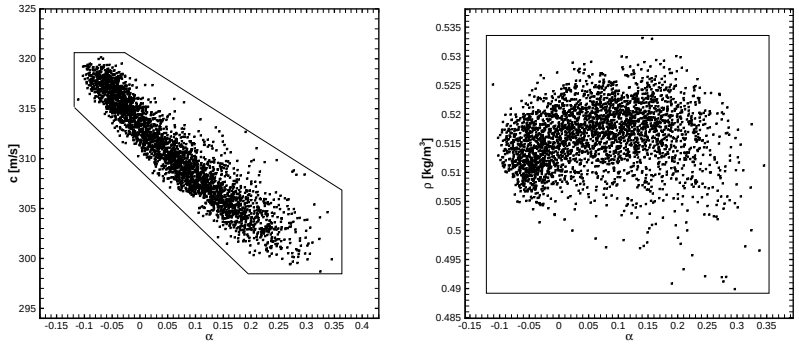

Figure 8. Input parameters - 9000 samples, Dodge City, 8200m

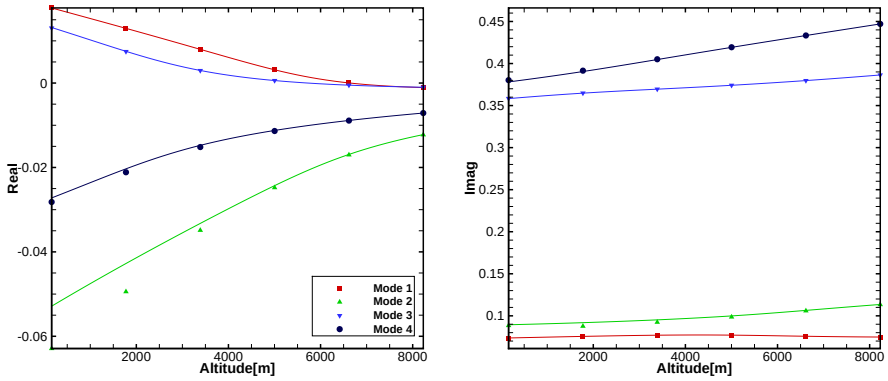

Figure 9. Goland Wing Mode Tracking - M0.90, $\alpha = 0°$

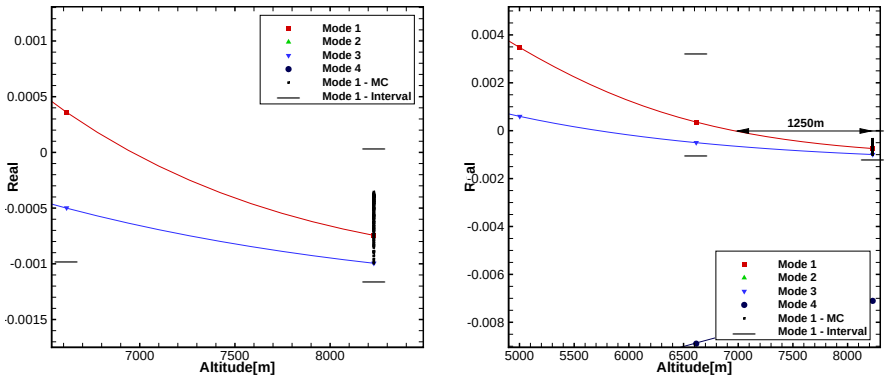

Figure 10. Goland Wing variability on Mode 1 Eigenvalue

altitude and location of the sample source, can decrease the stability margin by 1250m, as demonstrated in fig.10.

The histograms for the real and imaginary parts of the eigenvalue, using 1500 samples are shown in fig.11. The total range of the variation corresponds to ±40% of the mean value for the real part and ±2% for the imaginary component.

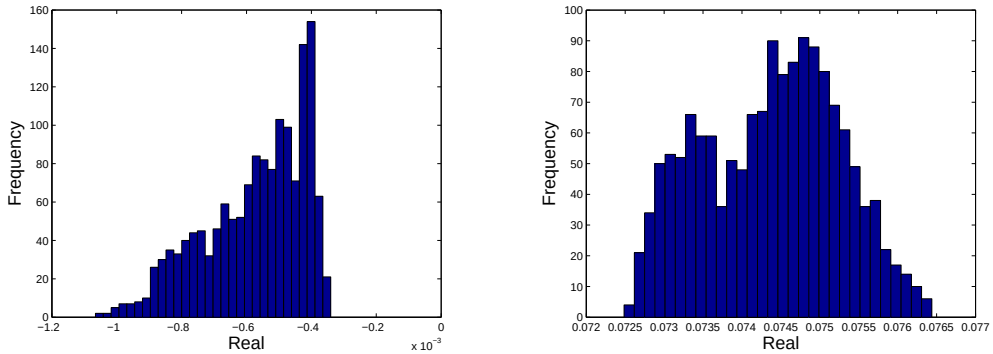

Figure 11. Eigenvalue Histogram

B. MDO Wing

The MDO wing is a commercial transport wing, with a span of 36 metres, designed to fly in the transonic regime.[22] The profile is a thick supercritical section. The geometry is summarised in fig.12. The structure is modelled as a wing box running down the central portion of the wing. The problems of mapping this reduced planform to the full planform CFD model are considered in Goura *et al.*.[23] The CFD grid used has 81 thousand points, fig.12. The eigenvalue formulation used in this paper was applied to the MDO wing in references.[1,4] In the current work eight modes are retained and the mapped modes which participate in the aeroelastic instability are shown in fig.13. Aerostatic structural effects are also included in these calculations, in the case of the MDO wing the structural deformation has a significant impact on the flutter point.[4]

Having demonstrated the interval analysis on the Goland Wing, the MDO wing provides a more realistic

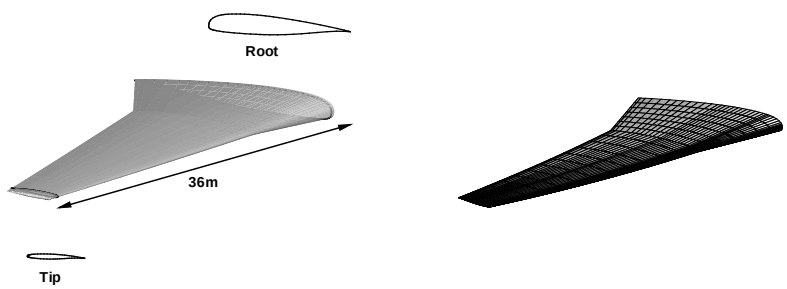

Figure 12. MDO Wing Geometry and CFD grid

structural configuration to study the impact of atmospheric variability. As shown in the eigenvalue analysis of the structure at ISA conditions, fig.14, the wing looses stability at about 4000m. Two altitudes were selected to conduct interval analysis, 4000m and 5500m. The data obtained from the Greenland station was used, since it shows a large amplitude on the measured quantities, the samples used to construct the interval constraints is shown in fig.15. The results obtained with the interval analysis are shown in fig.16. In the case of the MDO wing, the influence of the variability has a less dramatic impact on the loss of stability margin, here corresponds to approximately 500m. Table 5 shows the results from the maximisation process. Contrasting with the previous results, the MDO wing worst condition for flutter minimizes or reduces α. As

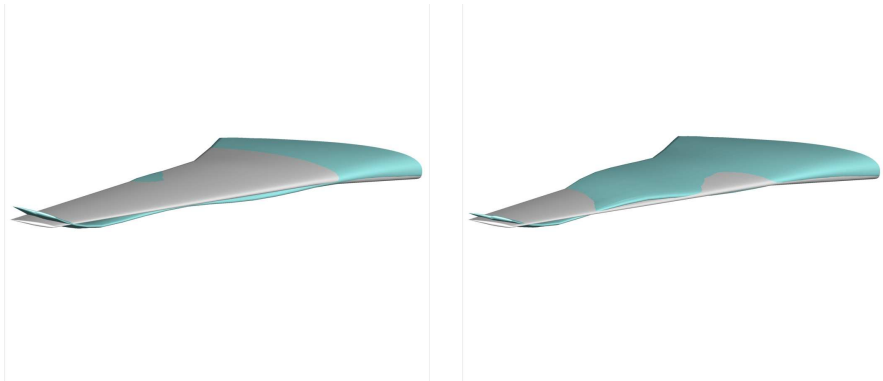

Figure 13. MDO Wing mode 1 and mode 2

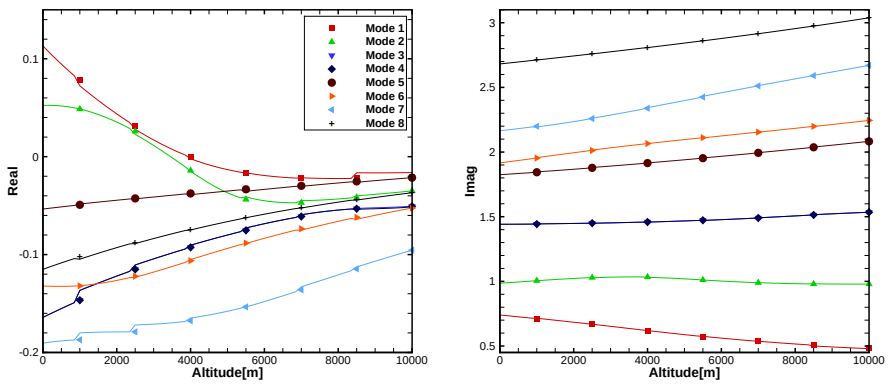

Figure 14. Mode tracking - MDO Wing, M=0.85, $\alpha = 1^\circ$

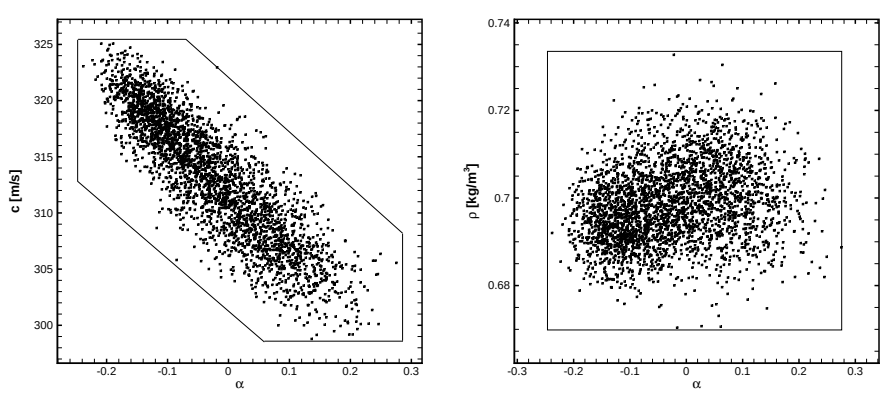

Figure 15. Interval set up for flutter analysis input parameters - Greenland, 5500m

shown in reference,[4] as density increases the wing tip nose down twist increases, after a certain altitude the wing tip twist starts to generate negative lift and the wing bends downwards. This has the effect of reducing the stability margin. Reducing the angle of attack of the wing has the effect of increasing the net tip twist angle, leading to an increase in negative load in this region.

Parameter	4000m	5000m
c [m/s]	328	322
$\rho[kg/m^3]$	0.86	0.73
α [deg.]	0.88°	0.84°

Table 5. Parameters for maximisation of flutter

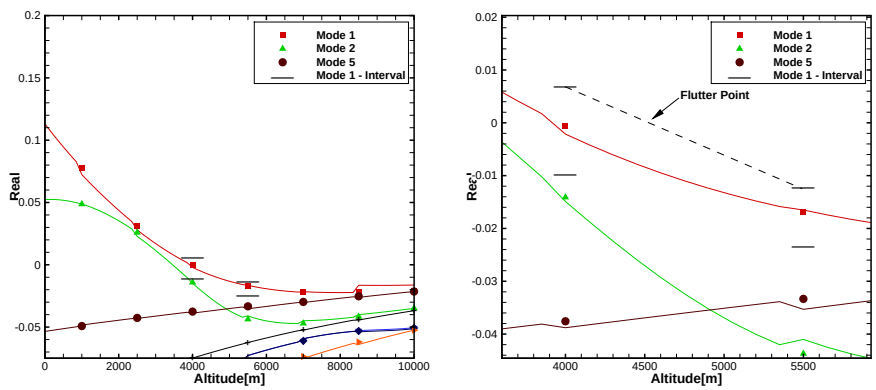

Figure 16. MDO Wing variability on Mode 1 Eigenvalue

VII. Conclusion

An approach to propagate atmospheric variability into aeroelastic stability analysis, using measurements and flight dynamics analysis has been investigated. From the initial atmospheric measurements, a flight dynamics set of tools have been employed to generate suitable input parameters for flutter calculations using CFD level aerodynamics and an eigenvalue based method. Parameters calculated from the flight dynamics analysis, α, exhibit a high degree of correlation with the speed of sound.

The statistical variability observed in the atmosphere for quantities such as temperature and density changes significantly with global location and altitude. Furthermore, these two quantities can also exhibit some degree of correlation. The practicality of using ISA conditions is unquestionable, however these conditions often don't even correspond to the mean of measured values. An adaptation of the interval method was used to represent the relation between input parameters. The interval method provided conservative estimates on the impact of the atmospheric variability. The loss of stability margin due to atmospheric variability is not negligible. From the two test cases examined in this work, atmospheric quantities have a negative impact on the flutter stability when the wing loading increases, although this sounds obvious, the path taken to maximise wing loading may not be so evident, as exhibited by the MDO wing. Hence, the necessity to represent the correct physical effects of the density and temperature variations on trim states and the aeroelastic stability calculation, i.e. include aerostatic deformations.

VIII. Acknowledgements

This work is funded by the European Union for the Marie Curie Excellence Team ECERTA under contract MEXT-CT-2006 042383.

References

[1]Badcock, K.J. and Woodgate, M.A., Prediction of Bifurcation Onset of Large Order Aeroelastic Models, 49th Structural Dynamics and Materials Conference, Schaumberg, Illinois, May, 2008, AIAA-2008-1820.

[2]Atmospheric Soundings, http://weather.uwyo.edu/upperair/sounding.html, (accessed 09.12.09)

[3]Marques, S., Badcock, K.J., Khodaparast, H.H. and Mottershead, J.E., Transonic Aeroelastic Stability Predictions Under the Influence of Structural Variability, Journal of Aircraft, vol.47 no.4 (1229-1239), 2010

[4]Marques, S., Badcock, K.J., Khodaparast, H.H. and Mottershead, J.E., On How Structural Model Variability Influences Transonic Aeroelastic Stability, AIAA-2010-3047, 51st AIAA/ASME/ASCE/AHS/ASC Structures, Structural Dynamics, and Materials Conference, Orlando, Florida, Apr. 12-15, 2010

[5]Badcock, K.J., M.A. Woodgate, M.A. and Richards, B.E., The Application of Sparse Matrix Techniques for the CFD based Aeroelastic Bifurcation Analysis of a Symmetric Aerofoil, AIAA Journal, 42(5), 883-892, May, 2004.

[6]Badcock, K.J., Woodgate, M.A. and Richards, B.E., Direct Aeroelastic Bifurcation Analysis of a Symmetric Wing Based on the Euler Equations, Journal of Aircraft, 42(3),731-737, 2005.

[7]Tobak, M. and Schiff, L. B., Aerodynamic Mathematical Modeling: Basic Concepts, AGARD Lecture Series on Dynamic Stability Parameters, Lecture No. 1, March 1981.

[8]Tobak, M., Chapman, G. T., and Schiff, L. B., Mathematical Modeling of the Aerodynamic Characteristics in Flight Dynamics, NASA technical report TM-85880, NASA, 1984.

[9]Gottlieb, D., Hussaini, M. Y., and Orszag, S. A., Theory and Applications of Spectral Methods, Spectral Methods for PDEs, Society for Industrial and AppliedMathematics, Philadelphia, 1984

[10]Canuto, C., Hussaini, M. Y., Quarteroni, A., and Zang, T. A., Spectral Methods in Fluid Dynamics,Springer- Verlag, New York, 1988.

[11]Elnagar, J., Kazemi, M. A., and Razzaghi, M., The Pseudospectral Legendre Method for Discretizing Optimal Control Problems, IEEE Transactions on Automatic Control, Vol. 40, No. 10, pp. 1793 1796, 1995

[12]Etkin, B., Dynamics of Flight, Stability and Control, 2nd Edition, Wiley, 1982

[13]Steven, B.L. and Lewis, F. L., Aircraft Control and Simulatoon, Wiley, 1992

[14]Ross, I.M., and Fahroo, F., User's Manual for DIDO 2002: a MatLab application package for dynamic optimisations, NPS Technical Rep., Dept. of Aeronautics and Astronautics, Naval Postrgraduate School, Monterery, CA, AA-02-002, 2002

[15]Ghoreyshi, M., Badcock, K. and Woodgate, M., Accelerating the Numerical Generation of Aerodynamic Models for Flight Simulation Journal of Aircraft, 46(3), 2009, DOI: 10.2514/1.39626

[16]Ghoreyshi, M., Badcock, K., Ronch, A., Marques, S., Swift, A., Ames N., Framework for establishing the limits of tabular aerodynamic models for flight dynamics analysis, AIAA Journal of Aircraft, (to appear), 2010.

[17]Vallespin, D., Badcock, K.J., Ghoreyshi, M., Da Ronch, A., Vos, J., Hitzelk, S., Simulation of Aircraft Manoeuvres Based On Computational Fluid Dynamics, AIAA-2010-8239, AIAA Atmospheric Flight Mechanics Conference, Toronto, Canada, 2-5 August, 2010.

[18]Cook, M. , V., Flight Dynamics Principles, second edition, Elsevier Aerospace Engineering Series, 2007

[19]Thompson, D., Wallace, J., Annular Modes in the Extratropical Circulation. Part I: Month-to-Month Variability, Journal of Climate, vol.13, 1000-1016, 2000.

[20]Beran, P.S., Knot, N.S., Eastep, F.E., Synder, R.D. and Zweber, J.V., Numerical Analysis of Store-Induced Limit Cycle Oscillarion, Journal of Aircraft, 41(6), 1315-1326, 2004.

[21]Bekas, K. and Saad, Y., "Computation of Smallest Eigenvalues using Spectral Schur Complements", *SIAM Journal of Scientific Computing*, Vol. 27, No. 2, 2005, pp. 458-481.

[22]Girodroux-Lavigne, P., Grisval, J. P., Guillemot, S., Henshaw, M., Karlsson, A., Selmin, V., Smith, J., Teupootahiti, E. and Winzell, B., "Comparison of static and dynamic fluid-structure interaction solutions in the case of a highly flexible modern transport aircraft wing", *Aerospace Science and Technology*, 7, 2003, 121-133.

[23]Goura, G.S.L., Badcock, K.J. and Woodgate, M.A., "Extrapolation Effects on Coupled Computational Fluid Dynamics/Computational Structural Dynamics Simulations", *AIAA Journal*, Vol. 41, No. 2, February, 2003, 312-314.